14th U.S. National Congress of Theoretical and Applied Mechanics
Blacksburg, VA, June 23–28, 2002

SPACECRAFT RELATIVE ORBIT GEOMETRY DESCRIPTION THROUGH ORBIT ELEMENT DIFFERENCES

Hanspeter Schaub*
ORION International Technologies, Albuquerque, NM 87106

The relative orbit geometry of a spacecraft formation can be elegantly described in terms of a set of orbit element differences relative to a common chief orbit. For the non-perturbed orbit motion these orbit element differences remain constant if the anomaly difference is expressed in terms of mean anomalies. A general method is presented to estimate the linearized relative orbit motion for both circular and elliptic chief reference orbits. The relative orbit is described purely through relative orbit element differences, not through the classical method of using Cartesian initial conditions. Analytical solutions of the relative motion are provided in terms of the true anomaly angle. By sweeping this angle from 0 to 2π, it is trivial to obtain estimates of the along-track, out-of-plane and orbit radial dimensions which are dictated by a particular choice of orbit element differences. The main assumption being made in the linearization is that the relative orbit radius is small compared to the Earth relative orbit radius. The resulting linearized relative motion solution can be used for both formation flying control applications or to assist in selecting the orbit element differences that yield the desired relative orbit geometry.

Introduction

The relative orbits within a spacecraft formation are typically prescribed through sets of Cartesian coordinate initial conditions in the rotating Hill reference frame.[1–4] The six Cartesian initial conditions are the invariant parameters of the relative orbit. However, to solve for the relative orbit motion that will result from such initial conditions, the differential equations of motion must be solved. Except for the unperturbed circular reference (or chief) orbit special case, solving the differential equations for the resulting relative motion analytically is a very challenging task that has been tackled in various papers. Melton develops in Reference 5 a state transition matrix that can be used to predict the relative motion for chief orbits with small eccentricities. Tschauner and Hempel have solved the relative equations of motion directly for the general case of having an elliptic chief orbit.[6] However, their solution is not explicit and requires the computation of an integral. Kechichian develops in Reference 1 the analytical solution to the relative orbit motion under the influence of both the J_2 and J_3 zonal harmonics assuming that the eccentricity is a very small parameter. Unfortunately these methods yield relatively complex solutions and the six Cartesian relative motion initial conditions do not easily reveal the nature of the resulting relative orbit. It is not intuitive to the relative orbit design process how to adjust the initial Cartesian conditions to obtain a relative orbit of the desired shape and size. More recently, Broucke has presented in Reference 7 an analytical solution to the linearized relative equations of motion for eccentric chief orbits. His solution uses both time and true anomaly and finds the current Cartesian coordinates of a deputy satelite given the initial Cartesian coordinates.

An alternate set of six invariant parameters to describe the relative orbit is to use orbit element differences relative to the chief orbit.[8–12] In References 8 and 9 the anomaly difference is prescribed in terms of the mean anomalies, not true or eccentric anomaly. The reason being that for elliptic motions, a mean anomaly difference between two satellites remains constant under the assumption of classical Keplerian two-body motion. Prescribing the relative orbit geometry through sets of relative orbit element differences has the major advantage that these relative orbit coordinates are constants of the non-perturbed orbit motion. Even if perturbations are considered, they typically have a similar influence on each of the satellites in the formation if these satellites are of equal build and type. For example, atmospheric drag will cause the orbits to decay. However, all satellites in the formation will experience nearly identical amounts of drag. As such, the *relative motion* between the satellites is only minorly affected by this perturbation. Further, as the orbits decay and the orbit elements such as the semi-major axis change, the orbit element differences which determine the relative motion will only vary slowly.

Using orbit element differences in the control of a spacecraft formation has advantages too. At any instant it is possible to map the current inertial position and velocities vectors into an equivalent set of orbit elements. By differencing the orbit elements of the deputy satellite to those of the chief satellite, we are able to compare these differences to the prescribed orbit element differences and determine any relative orbit errors. Note that no differential equations have to be solved to determine any relative orbit tracking errors. Several relative orbit control strategies have recently been suggested that feed back orbit errors in terms of orbit element differences.[13–17] On the other hand, using Cartesian coordinates to describe the desired relative orbit requires solving the nonlinear differential relative equations of motion of the desired relative orbit and differencing these states with the current position and velocity states, unless the control tolerances allow any of the linearized relative motion solutions to be used. Using the orbit element difference description we are not required to perform any linearization or solve any nonlinear differential equations to find the current desired deputy satellite position.

In References 16 and 18, a linearized mapping is presented between a particular set of orbit element differences and the Cartesian position and velocity coordinates in the rotating Hill reference frame. This work was then expanded in Reference 19 to provide the state transition matrix for the relative orbit motion using orbit elements. This paper expands on this theory and develops direct relationships between the orbit element differences and the resulting relative orbit geometry for both circular and eccentric chief orbits. In particular, the relative orbit along-track, out-of-plane and orbit radial dimensions are estimated for specific sets of orbit element differences. Contrary to previous work in this area,[11,12] the presented results apply to both circular and elliptic chief orbits. But more generally, analytic solutions are provided for the linearized relative orbit motion, where the linearizing assumption is that the relative orbit radius is small compared to the inertial orbit radius. While Tschauner and Hempel provide the complex solution of the true differential equations of motion, the linearized analytical solution here is obtained from geometric arguments without solving any differential equations. The resulting linearized analytic relative orbit solution is useful when designing a relative orbit that must meet scientific mission requirements. If the relative orbit must have a certain along-track behavior, then this solution directly shows how to adjust the relative orbit element differences to achieve the desired motion. Further, the general solution for elliptic chief orbits is specialized for the small eccentricity and near

*Aerospace Research Engineer, AIAA and AAS Member.

circular orbit case. With the small eccentricity case, linear terms in the eccentricity e are retained, while higher order terms of e are dropped. The near-circular analysis drops any terms containing e. The linearized relationship between the orbit element difference description of the relative orbit and the classical Cartesian coordinate description is usefull in both designing and controlling relative orbits in terms of orbit element differences.

Relative Orbit Definitions

To following nomenclature is adopted to describe the satellites within a formation. The satellite about which all other satellites are orbiting is referred to as the chief satellite. The remaining satellites, referred to as the deputy satellites, are to fly in formation with the chief. Note that it is not necessary that the chief position actually be occupied by a physical satellite. Sometimes this chief position is simply used as an orbiting reference point about which the deputy satellites orbit. To express how the relative orbit geometry is seen by the chief, we introduce the Hill coordinate frame $\mathcal{O}$.[20] Its origin is at the osculating chief satellite position and its orientation is given by the vector triad $\{\hat{\boldsymbol{o}}_r, \hat{\boldsymbol{o}}_\theta, \hat{\boldsymbol{o}}_h\}$ shown in Figures 1. The unit vector $\hat{\boldsymbol{o}}_r$ is in the orbit radius direction, while $\hat{\boldsymbol{o}}_h$ is parallel to the orbit momentum vector in the orbit normal direction. The unit vector $\hat{\boldsymbol{o}}_\theta$ then completes the right-handed coordinate system. Let $\boldsymbol{r}$ be the chief orbit radius and $\boldsymbol{h}$ be the chief angular momentum vector. Unless noted otherwise, any non-differenced states or orbit elements are assumed to be those of the chief. Differenced states are assumed to be differences between the deputy and chief satellite. Mathematically, these $\mathcal{O}$ frame orientation vectors are expressed as

$$\hat{\boldsymbol{o}}_r = \frac{\boldsymbol{r}}{r} \tag{1a}$$

$$\hat{\boldsymbol{o}}_\theta = \hat{\boldsymbol{o}}_h \times \hat{\boldsymbol{o}}_r \tag{1b}$$

$$\hat{\boldsymbol{o}}_h = \frac{\boldsymbol{h}}{h} \tag{1c}$$

with $\boldsymbol{h} = \boldsymbol{r} \times \dot{\boldsymbol{r}}$. Note that if the inertial chief orbit is circular, then $\hat{\boldsymbol{o}}_\theta$ is parallel to the satellite velocity vector.

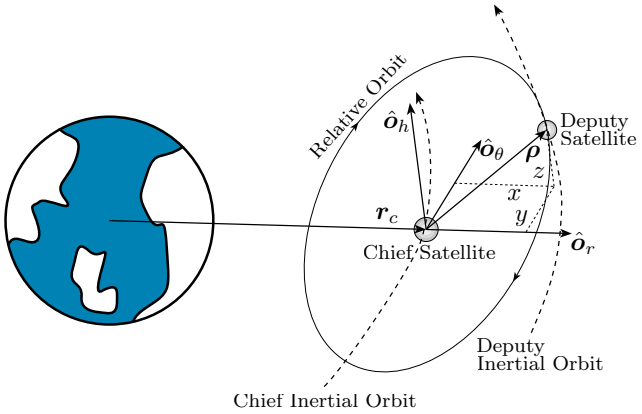

Fig. 1 Illustration of a General Type of Spacecraft Formation with Out-Of-Plane Relative Motion

The relative orbit position vector $\boldsymbol{\rho}$ and velocity vector $\dot{\boldsymbol{\rho}}$ of a deputy satellite relative to the chief is expressed in Cartesian $\mathcal{O}$ frame components as

$$\boldsymbol{\rho} = (x, y, z)^T \tag{2}$$

$$\dot{\boldsymbol{\rho}} = (\dot{x}, \dot{y}, \dot{z})^T \tag{3}$$

The relative position and velocity vectors are compactly written as

$$\boldsymbol{X} = \begin{pmatrix} \boldsymbol{\rho} \\ \dot{\boldsymbol{\rho}} \end{pmatrix} \tag{4}$$

Thus, given both the relative position vector $\boldsymbol{\rho}$ and the chief position vector $\boldsymbol{r}$, we are able to determine the inertial motion of a deputy satellite.

Instead of using Cartesian coordinates to describe the relative position of a deputy to the chief, we can also use orbit element differences.[8,9] Let the vector $\boldsymbol{e}$ be defined through the orbit elements

$$\boldsymbol{e} = (a, \theta, i, q_1, q_2, \Omega)^T \tag{5}$$

where a is the semi-major axis, $\theta = \omega + f$ is the true latitude angle, i is the orbit inclination angle, Ω is the argument of the ascending node and q_i are defined as

$$q_1 = e\cos\omega \tag{6}$$

$$q_2 = e\sin\omega \tag{7}$$

The parameter e is the eccentricity, ω is the argument of perigee, and f be the true anomaly. Let the relative orbit be described through the orbit element difference vector $\delta\boldsymbol{e}$. Whereas all six elements of the relative orbit state $\boldsymbol{X}$ vector are time varying, all the orbit element differences, except for the true anomaly difference, are constant for a non-perturbed Keplerian orbit. This has many advantages when measuring the relative orbit error motion and applying it to a control law. In References 18 and 16 a convenient direct mapping is presented which translates between the Cartesian states $\boldsymbol{X}$ and the orbit element differences $\delta\boldsymbol{e}$. In deriving this mapping, it is assumed that the relative orbit radius ρ is small in comparison to the inertial chief orbit radius r. While Reference 16 shows both the forward and backward mapping between these relative orbit coordinates, only the mapping from orbit element differences to Cartesian Hill frame coordinates is used in the following development. The relative position vector components are given in terms of orbit elements through:

$$\begin{aligned} x \approx{}& \frac{r}{a}\delta a + \frac{V_r}{V_t} r\ \delta\theta - \frac{r}{p}(2aq_1 + r\cos\theta)\delta q_1 \\ &- \frac{r}{p}(2aq_2 + r\sin\theta)\delta q_2 \end{aligned} \tag{8a}$$

$$y \approx r(\delta\theta + \cos i\ \delta\Omega) \tag{8b}$$

$$z \approx r(\sin\theta\ \delta i - \cos\theta\sin i\ \delta\Omega) \tag{8c}$$

The parameter $p = a(1-e^2) = a\eta^2$ is the semi-latus rectum, with $\eta = \sqrt{1-e^2}$ being another convenient measure of the orbit eccentricity. The chief radial and transverse velocity components V_r and V_t are defined as

$$V_r = \dot{r} = \frac{h}{p}(q_1\sin\theta - q_2\cos\theta) \tag{9}$$

$$V_t = r\dot{\theta} = \frac{h}{p}(1 + q_1\cos\theta + q_2\sin\theta) \tag{10}$$

The orbit radius r is defined in terms of the orbit elements used in Eq. (5) as

$$r = \frac{a(1-q_1^2-q_2^2)}{1 + q_1\cos\theta + q_2\sin\theta} = \frac{a\eta^2}{1 + e\cos f} \tag{11}$$

Note that the ratio V_r/V_t in Eq. (8a) can be rewritten as

$$\frac{V_r}{V_t} = \frac{q_1\sin\theta - q_2\cos\theta}{1 + q_1\cos\theta + q_2\sin\theta} = \frac{e\sin f}{1 + e\cos f} \tag{12}$$

Alternate mappings between orbit element differences and Cartesian relative orbit coordinates are found in References 10 and 21.

General Elliptic Orbits

Note that Eq. 8 provides us a direct linear mapping between orbit element differences $\delta\boldsymbol{e}$ and the Hill frame

Cartesian coordinates $\boldsymbol{\rho}$. The only linearizing assumption that was made is that the relative orbit radius ρ is small compared to the inertial chief orbit radius r. However, when describing a relative orbit through orbit element differences, it is not convenient to describe the anomaly difference through $\delta\theta$ or δf. For elliptic chief orbits, the difference in true anomaly between two orbits will vary with time. To avoid this issue, the desired anomaly difference between two orbits is expressed in terms of a mean anomaly difference δM. This anomaly difference will remain constant, assuming unperturbed Keplerian motion, even if the chief orbit is elliptic. To express the mean anomaly differences in terms of other anomaly differences, we make use of the mean anomaly definition

$$M = E - e\sin E \tag{13}$$

where E is the eccentric anomaly. Taking its first variation we express differences in mean anomaly in terms of differences in eccentric anomaly and differences in eccentricity.

$$\begin{aligned}\delta M &= \frac{\partial M}{\partial E}\delta E + \frac{\partial M}{\partial e}\delta e \\ &= (1 - e\cos E)\delta E - \sin E\delta e\end{aligned} \tag{14}$$

Using the mapping between eccentric anomaly E and true anomaly f

$$\tan\frac{f}{2} = \sqrt{\frac{1+e}{1-e}}\tan\frac{E}{2} \tag{15}$$

and taken its first variation, differences in E are then expressed as differences in f and e through

$$\delta E = \frac{\eta}{1+e\cos f}\delta f - \frac{\sin f}{1+e\cos f}\frac{\delta e}{\eta} \tag{16}$$

Substituting Eq. (16) into Eq. (14) and making use of the orbit identities

$$(1 - e\cos E) = \frac{\eta^2}{(1+e\cos f)} \tag{17}$$

$$\sin E = \frac{\eta\sin f}{(1+e\cos f)} \tag{18}$$

the desired relationship between differences in true and mean anomalies is found.

$$\delta f = \frac{(1+e\cos f)^2}{\eta^3}\delta M + \frac{\sin f}{\eta^2}(2 + e\cos f)\delta e \tag{19}$$

Let us redefine the orbit element difference vector $\delta\boldsymbol{e}$ to consist of

$$\delta\boldsymbol{e} = (\delta a, \delta M, \delta i, \delta\omega, \delta e, \delta\Omega)^T \tag{20}$$

Note that all these orbit element differences are constants for Keplerian two-body motion. Further, while using q_1 and q_2 instead of e and ω allows us to avoid singularity issues for near-circular orbits, for the following relative orbit geometry discussion such singularities do not appear. In fact, describing the relative orbit path using δe and $\delta\omega$ instead of δq_1 and δq_2 yields a simpler and more elegant result. Using Eqs. (6) and (7), the differences in the q_i parameters are expressed as

$$\delta q_1 = \cos\omega\delta e - e\sin\omega\delta\omega \tag{21a}$$

$$\delta q_2 = \sin\omega\delta e + e\cos\omega\delta\omega \tag{21b}$$

After substituting Eqs. (19) and (21) into the linear mapping in Eq. (8) and simplifying the result, we are able to express the relative position coordinates (x, y, z) in terms of the orbit element differences in Eq. (20) through

$$x(f) \approx \frac{r}{a}\delta a + \frac{ae\sin f}{\eta}\delta M - a\cos f\delta e \tag{22a}$$

$$\begin{aligned}y(f) \approx{}& \frac{r}{\eta^3}(1+e\cos f)^2\delta M + r\delta\omega \\ &+ \frac{r\sin f}{\eta^2}(2+e\cos f)\delta e + r\cos i\delta\Omega\end{aligned} \tag{22b}$$

$$z(f) \approx r(\sin\theta\delta i - \cos\theta\sin i\delta\Omega) \tag{22c}$$

Note that with this linearized mapping the difference in the argument of perigee $\delta\omega$ does not appear in the $x(f)$ expression. Further, these equations are valid for both circular and elliptic chief orbits. Only the δM and δe terms contribute periodic terms to the radial x solution. Due to the dependence of r on the true anomaly f, all orbit element difference terms in the along-track y motion contribute both static offsets as well as periodic terms. For the out-of-plane z motion both the δi and $\delta\Omega$ terms control the out-of-plane oscillations. By dividing the dimensional (x, y, z) expressions in Eq. (22) by the chief orbit radius r and making use of Eq. (11), we obtain the non-dimensional relative orbit coordinates (u, v, w).

$$\begin{aligned}u(f) \approx{}& \frac{\delta a}{a} + (1+e\cos f)\frac{e\sin f}{\eta^3}\delta M \\ &- \frac{(1+e\cos f)}{\eta^2}\cos f\delta e\end{aligned} \tag{23a}$$

$$\begin{aligned}v(f) \approx{}& (1+e\cos f)^2\frac{\delta M}{\eta^3} + \delta\omega \\ &+ \frac{\sin f}{\eta^2}(2+e\cos f)\delta e + \cos i\delta\Omega\end{aligned} \tag{23b}$$

$$w(f) \approx \sin\theta\delta i - \cos\theta\sin i\delta\Omega \tag{23c}$$

Since $(y, z) \ll r$, the non-dimensional coordinates (v, w) are the angular deputy satellite relative orbit position with respect to the chief orbit radius axis.

However, the present form of Eq. (23) is not convenient to determine the overall non-dimensional shape of the relative orbit. Reason is that there are several sin() and cos() functions being added here. Using the identities

$$\begin{aligned}A\sin t + B\cos t &= \sqrt{A^2+B^2}\cos\left(t - \tan^{-1}\left(\frac{A}{B}\right)\right) \\ &= -\sqrt{A^2+B^2}\sin\left(t - \tan^{-1}\left(\frac{B}{-A}\right)\right)\end{aligned} \tag{24}$$

as well as standard trigonometric identities, we are able to rewrite the linearized non-dimensional relative orbit motion as

$$\begin{aligned}u(f) \approx{}& \frac{\delta a}{a} + \frac{1}{\eta^2}\sqrt{\frac{e^2\delta M^2}{\eta^2} + \delta e^2}\cos(f - f_u) \\ &- \frac{e\delta e}{2\eta^2} + \frac{e}{2\eta^2}\sqrt{\frac{e^2\delta M^2}{\eta^2} + \delta e^2}\cos(2f - f_u)\end{aligned} \tag{25a}$$

$$\begin{aligned}v(f) \approx{}& \left(\left(1 + \frac{e^2}{2}\right)\frac{\delta M}{\eta^3} + \delta\omega + \cos i\delta\Omega\right) \\ &+ \frac{2}{\eta^2}\sqrt{\frac{e^2\delta M^2}{\eta^2} + \delta e^2}\cos(f - f_v) \\ &+ \frac{e}{2\eta^2}\sqrt{\frac{e^2\delta M^2}{\eta^2} + \delta e^2}\cos(2f - f_v)\end{aligned} \tag{25b}$$

$$w(f) \approx \sqrt{\delta i^2 + \sin^2 i\delta\Omega^2}\cos(\theta - \theta_w) \tag{25c}$$

with the phase angles f_u, f_v and θ_w being defined as

$$f_u = \tan^{-1}\left(\frac{e\delta M}{-\eta\delta e}\right) \tag{26a}$$

$$f_v = \tan^{-1}\left(\frac{\eta\delta e}{e\delta M}\right) = f_u - \frac{\pi}{2} \tag{26b}$$

$$\theta_w = \tan^{-1}\left(\frac{\delta i}{-\sin i\ \delta\Omega}\right) \tag{26c}$$

At these phase angles, the trigonometric terms will reach either their minimum or maximum value. Note that 180 degrees can be added or subtracted from these angles to yield the second extrema point of the trigonometric functions. To further reduce the expression in Eq. (25), let us introduce the small states δ_u and δ_w:

$$\delta_u = \sqrt{\frac{e^2\delta M^2}{\eta^2} + \delta e^2} \tag{27a}$$

$$\delta_w = \sqrt{\delta i^2 + \sin^2 i\delta\Omega^2} \tag{27b}$$

Using these δ_u and δ_w definitions as well as Eq. (26b), the linearized relative orbit motion is described through

$$\begin{aligned} u(f) \approx{}& \frac{\delta a}{a} - \frac{e\delta e}{2\eta^2} \\ &+ \frac{\delta_u}{\eta^2}\left(\cos(f-f_u) + \frac{e}{2}\cos(2f-f_u)\right) \end{aligned} \tag{28a}$$

$$\begin{aligned} v(f) \approx{}& \left(\left(1+\frac{e^2}{2}\right)\frac{\delta M}{\eta^3} + \delta\omega + \cos i\delta\Omega\right) \\ &- \frac{\delta_u}{\eta^2}\left(2\sin(f-f_u) + \frac{e}{2}\sin(2f-f_u)\right) \end{aligned} \tag{28b}$$

$$w(f) \approx \delta_w \cos(\theta - \theta_w) \tag{28c}$$

Note that the $\cos(2f)$ and $\sin(2f)$ terms are multiplied by the eccentricity e. Only if the chief orbit is very eccentric will these terms have a significant contribution to the overall relative orbit dimension. For the more typical case of having a chief orbit with a small eccentricity e, these terms only provide small perturbations to the dominant $\sin(f)$ and $\cos(f)$ terms. Using Eq. (28), it is trivial to determine the maximum radial, along-track and out-of-plane dimension of a relative orbit provided that the relative orbit geometry is prescribed through the set of orbit element differences $\{\delta a, \delta e, \delta i, \delta\Omega, \delta\omega, \delta M\}$. Note that this linearized relative orbit motion is valid for both circular and elliptic chief reference orbits. The only linearizing assumption made so far is that the relative orbit radius is small compared to the planet centric inertial orbit radius. However, note that we are only estimating the non-dimensional relative orbit shape. To obtain the true radial, along-track and out-of-plane motions, we need to mulitpy (u, v, w) by the chief orbit radius r. Since r is time dependent for an elliptic chief orbit, the points of maximum angular separation between deputy and chief satellites may not correspond to the point of maximum physical distance. To plot the dimensional linearized relative orbit motion, we use Eq. (22) instead. However, due to the ratio's of sin() and cos() terms, it is not trivial to obtain the maximum physical dimensions of the relative orbit.

Let us take a closer look at the out-of-plane motion. The true latitude angle θ_w, at which the maximum angular out-of-plane motion will occur, is given by Eq. (26c). As expected, if only a $\delta\Omega$ is prescribed, then the maximum w motion occurs during the equator crossing at $\theta = 0$ or 180 degrees. If only a δi is prescribed, then the maximum w motion occurs at $\theta = \pm 90$ degrees.

The maximum angular out-of-plane motion is given by the angle δ_w as shown in Figure 2. This angle δ_w is the tilt angle of the deputy orbit plane relative to the chief orbit plane. As such, it is the angle between the angular momentum vector

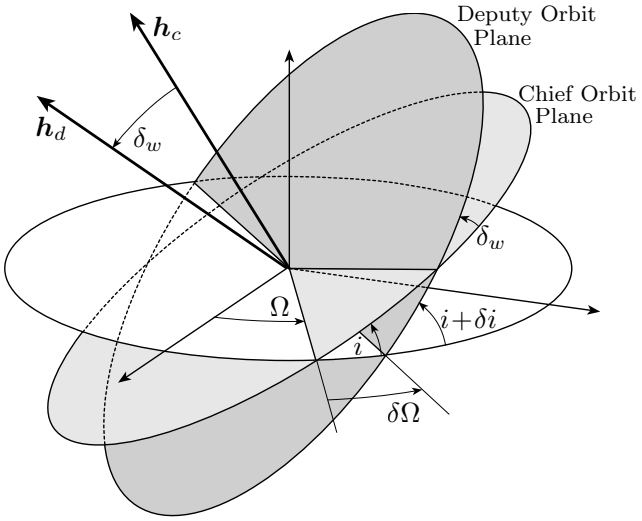

Fig. 2 Illustration of Orbit Plane Orientation Difference between Chief and Deputy Satellites

of the chief orbit and the angular momentum vector of the deputy orbit. To prove that δ_w is indeed this angle, let us make use of the spherical law of cosines for angles. Using the spherical trigonometric law of cosines, we are able to relate the angles $\delta\Omega$, i, δi and δ_w through:[22]

$$\cos\delta_w = \cos i\cos(i+\delta i) + \sin i\sin(i+\delta i)\cos\delta\Omega \tag{29}$$

Assuming that $\delta\Omega$, δi and δ_w are small angles, we approximate $\sin x \approx x$ and $\cos x \approx 1 - x^2/2$ to solve for δ_w.

$$\delta_w = \sqrt{\delta i^2 + \sin^2 i\delta\Omega^2} \tag{30}$$

Using the angle δ_w, the out-of-plane motion $w(f)$ in Eq. (28c) is written in the compact form shown.[12,23]

Chief Orbits with Small Eccentricity

In this section we assume that the chief orbit eccentricity e is a small quantity. In particular, we assume that e is small but greater than ρ/r, while powers of e are smaller than ρ/r. In this case we only retain terms which are linear in e and drop higher order terms of e. The orbit radius r is now approximated as

$$r = \frac{a\eta^2}{1+e\cos f} \approx a(1-e\cos f) \tag{31}$$

while $\eta^2 \approx 1$. The linearized dimensional relative orbit motion in Eq. (22) is written for the small eccentricity case as:

$$\begin{aligned} x(f) \approx{}& (1-e\cos f)\delta a + \frac{ae\sin f}{\eta}\delta M \\ &- a\cos f\delta e \end{aligned} \tag{32a}$$

$$\begin{aligned} y(f) \approx{}& \frac{a}{\eta}(1+e\cos f)\delta M + a(1-e\cos f)\delta\omega \\ &+ a\sin f(2-e\cos f)\delta e \\ &+ a(1-e\cos f)\cos i\delta\Omega \end{aligned} \tag{32b}$$

$$z(f) \approx a(1-e\cos f)(\sin\theta\delta i - \cos\theta\sin i\delta\Omega) \tag{32c}$$

Making use of the trigonometric identity in Eq. (24), the (x, y, z) motion is written as

$$x(f) \approx \delta a + a\delta_x \cos(f - f_x) \tag{33a}$$

$$y(f) \approx a\left(\frac{\delta M}{\eta} + \delta\omega + \cos i\delta\Omega\right) - a\delta_y \sin(f - f_y) - \frac{ae}{2}\sin(2f)\delta e \tag{33b}$$

$$z(f) \approx a\delta_z \cos(\theta - \theta_z) - \frac{ae}{2}\delta_z \cos(2f - f_z) - \frac{ae}{2}\left(\sin\omega\delta i - \cos\omega \sin i\delta\Omega\right) \tag{33c}$$

with the small states δ_x, δ_y and δ_z defined as

$$\delta_x = \sqrt{\frac{e^2\delta M^2}{\eta^2} + \left(\delta e + \frac{\delta a}{a}\right)^2} \tag{34a}$$

$$\delta_y = \sqrt{4\delta e^2 + e^2\left(\frac{\delta M}{\eta} - \delta\omega - \cos i\delta\Omega\right)^2} \tag{34b}$$

$$\delta_z = \sqrt{\delta i^2 + \sin^2 i\delta\Omega^2} \tag{34c}$$

and the phase angles f_x, f_y, θ_z and f_z defined as

$$f_x = \tan^{-1}\left(\frac{e\delta M}{-\eta\left(\delta e + \frac{\delta a}{a}\right)}\right) \tag{35a}$$

$$f_y = \tan^{-1}\left(\frac{e\left(\frac{\delta M}{\eta} - \delta\omega - \cos i\delta\Omega\right)}{-2\delta e}\right) \tag{35b}$$

$$\theta_z = \tan^{-1}\left(\frac{\delta i}{-\sin i\delta\Omega}\right) \tag{35c}$$

$$f_z = \tan^{-1}\left(\frac{\cos\omega\delta i + \sin\omega\sin i\delta\Omega}{\sin\omega\delta i - \cos\omega\sin i\delta\Omega}\right) \tag{35d}$$

Note that the orbital radial motion $x(f)$ for the small eccentricity case is identical to the general orbit radial coordinate in Eq. (22a) if δa is zero. The semi-major axis difference must be zero for bounded relative motion if no perturbations are present. With perturbations present, δa may be non-zero and the orbit radial coordinate will then be different between the linearizing approximations. The estimated along-track motion $y(f)$ and out-of-plane motion $z(f)$ will always be numerically different between the generally elliptic case and the small eccentricity case.

The dimensional form of the relative orbit motion in Eq. (32) is convenient to determine the amplitudes of the sinusoidal motion in either the along-track, orbit radial or out-of-plane motion. Note that since e is considered small, the double-orbit frequency terms $\sin(2f)$ are only a minor perturbutation to the dominant orbit frequency sinusoidal terms.

Near-Circular Chief Orbit

If the chief orbit is circular or near-circular, then the linearized relative equations of motion are given through the famous Clohessy-Wiltshire or CW equations.[24] These are sometimes also referred to as Hill's equations.[20]

$$\ddot{x} - 2n\dot{y} - 3n^2 x = 0 \tag{36a}$$

$$\ddot{y} + 2n\dot{x} = 0 \tag{36b}$$

$$\ddot{z} + n^2 z = 0 \tag{36c}$$

Further, these differential equations are only valid if the relative orbit radius is small compared to the planet centric orbit radius. If the relative orbit initial conditions satisfy the constraint

$$\dot{y}_0 + 2nx_0 = 0 \tag{37}$$

then a bounded relative motion will occur. Assuming this constraint is satisfied, then the differential CW equations can now be solved for an analytical solution of the relative orbit motion.

$$x(t) = A_0 \cos(nt + \alpha) \tag{38a}$$

$$y(t) = -2A_0 \sin(nt + \alpha) + y_{off} \tag{38b}$$

$$z(t) = B_0 \cos(nt + \beta) \tag{38c}$$

The integration constants A_0, B_0, α, β and y_{off} are determined through the relative orbit initial conditions. These equations have been extensively used to generate relative orbits if the chief orbit is circular. Let us now compare the predicted (x, y, z) motion in terms of the true anomaly in Eq. (33) to the CW solution in Eq. (38) if the chief orbit is assumed to be near-circular (i.e. $e < \rho/r$). In this case terms containing the eccentricity e are dropped, as compared to the small eccentricity case studied earlier where only higher order terms of e were dropped. Assuming that all $\delta\boldsymbol{e}$ components are small (i.e. the relative orbit radius is assumed to be small compared to the inertial orbit radius), and letting $e \to 0$, we find that $r \to a$ and $\eta \to 1$. Further, note that f_x and f_y approach 0. Using Eq. (33) the relative orbit motion $(x(f), y(f), z(f))$ is expressed for the near-circular chief orbit special case as

$$x(f) \approx \delta a - a\cos f\delta e \tag{39a}$$

$$y(f) \approx a(\delta\omega + \delta M + \cos i\delta\Omega) + 2a\sin f\delta e \tag{39b}$$

$$z(f) \approx a\sqrt{\delta i^2 + \sin^2 i\delta\Omega^2}\cos(\theta - \theta_z) \tag{39c}$$

Note that the maximum width of the oscillatory along-track motion y is given by $2a\delta e$. This result has been previously presented in References 11 and 12. Comparing Eqs. (38) and (39) and noting that $nt = f$ for this case, we are able to establish a direct relationship between the CW constants and the orbit element differences.

$$A_0 = -a\delta e \tag{40a}$$

$$B_0 = a\sqrt{\delta i^2 + \sin^2 i\delta\Omega^2} \tag{40b}$$

$$\alpha = 0 \tag{40c}$$

$$\beta = \omega - \theta_z \tag{40d}$$

$$y_{off} = a(\delta\omega + \delta M + \cos i\delta\Omega) \tag{40e}$$

Recall that Eqs. (38) require that the bounded relative motion constraint is satisfied. Thus the δa term is set to zero when comparing the two forms of the relation orbit motion expression.

Prescribing Bounded Relative Motion Conditions

Eqs. (22), (28), (33) or (39) show how the orbit element differences and the Hill frame Cartesian coordinates must be related for any chief true anomaly angle f. Since this mapping must hold at any instance of time, however, these linearized equations also approximate a solution for the relative orbit motion $\boldsymbol{\rho}(t)$. To map between time and the true anomaly we must solve Kepler's equation. However, to be able to describe the relative orbit geometry in terms of the Hill frame Cartesian coordinates, the forms presented in Eqs. (22), (28), (33) or (39) in terms of the true anomaly f are preferred. The reason for this is that by sweeping f through a complete revolution, the (x, y, z) coordinates found through these equations will yield the linearized relative orbit approximation that results due to a prescribed set of constant orbit element differences. Note that no differential equations are solved here to determine the relative orbit motion, and that the dominant relative orbit radial (x-direction), along-track (y-direction) and out-of-plane motion (z-direction) can be trivially extracted.

However, note that Eqs. (22), (28), (33) or (39) do not explicitly contain any secular terms. For the classical two-body orbital motion, the only condition on two inertial orbits to have a closed relative orbit is that their orbit energies must be equal. In terms of orbit elements this corresponds to demanding that

$$\delta a = 0 \tag{41}$$

This constraint is valid for both circular and elliptical chief orbits. Also, note that this constraint is the precise requirement of the Keplerian motion for bounded relative orbit paths; no linearizations have been made here. For Keplerian two-body motion, all the orbit element differences will naturally remain constant except for the mean anomaly difference. If δa is not zero between two orbits, then these orbits will drift apart due to having different orbit periods. In this case δM will not remain a constant, but grow larger with time. The linearizations in Eqs. (22), (28), (33) or (39) can still be used to predict the relative orbit motion, but only until the relative orbit radius ρ is no longer small compared to the inerital chief orbit radius r.

Next we would like to see what conditions the $\delta a = 0$ constraint imposes on the initial Hill frame Cartesian coordinates $\boldsymbol{X}(t_0) = \boldsymbol{X}_0$. Let us use the inverse mapping between orbit element differences $\delta\boldsymbol{e}$ and the Hill frame Cartesian coordinates $\boldsymbol{X}$ found in Reference 16 to express δa as

$$\begin{aligned}\delta a = 0 = 2\alpha(2+3\kappa_1+2\kappa_2)x(t) + 2\alpha\nu(1-2\kappa_1+\kappa_2)y(t) \\ + \frac{2\alpha^2\nu p}{V_t}\dot{x}(t) + \frac{2a}{V_t}(1+2\kappa_1+\kappa_2)\dot{y}(t)\end{aligned} \tag{42}$$

where the parameters

$$\alpha = a/r \tag{43}$$

$$\nu = V_r/V_t \tag{44}$$

$$\kappa_1 = \alpha\left(\frac{p}{r} - 1\right) \tag{45}$$

$$\kappa_2 = \alpha\nu^2\frac{p}{r} \tag{46}$$

are used to simplify the expression. This general constraint can be further simplified by expressing it at the initial time, where t_0 is defined as the time where the true anomaly f is equal to zero and the satellite is at the orbit periapses. Note that the orbit radius is now given by

$$r(t_0) = r_p = a(1-e) \tag{47}$$

Further, the radial velocity V_r is given by

$$V_r(t_0) = \dot{r}(t_0) = \frac{h}{p}(q_1\sin\omega - q_2\cos\omega) = 0 \tag{48}$$

Thus, using Eqs. (44) and (46) we find that $\nu = 0$ and $\kappa_2 = 0$. The bounded relative orbit constraint equation is now written specifically at the initial time as

$$\begin{aligned}0 = 2\frac{a}{r_p}\left(2+3\frac{a}{r_p}\left(\frac{p}{r_p}-1\right)\right)x_0 \\ + 2\frac{a}{V_t(t_0)}\left(1+2\frac{a}{r_p}\left(\frac{p}{r_p}-1\right)\right)\dot{y}_0\end{aligned} \tag{49}$$

Since $V_t(t_0) = r_p\dot{\theta}_p$ and making use of Eq. (47), this constraint is further reduced to the simpler form

$$(2+e)x_0 + \frac{1}{\dot{\theta}_p}(1+e)\dot{y}_0 = 0 \tag{50}$$

Let $n = \sqrt{\mu/a^3}$ be the chief mean angular motion. Expressing the true latitude rate $\dot{\theta}$ at perigee as

$$\dot{\theta}_p = \frac{h}{r_p^2} = \frac{\sqrt{\mu p}}{a^2(1-e)^2} = n\sqrt{\frac{1+e}{(1-e)^3}} \tag{51}$$

the constraint is written in its final form as[25]

$$\frac{\dot{y}_0}{x_0} = \frac{-n(2+e)}{\sqrt{(1+e)(1-e)^3}} \tag{52}$$

Let us linearize this constraint about a small eccentricity. In this case terms which are linear in e are retained and higher order terms in e are dropped. The bounded relative motion constraint on the initial Cartesian coordinates is then given by

$$\dot{y}_0 + (2+3e)nx_0 = 0 \tag{53}$$

The find the initial Cartesian coordinates constraint for bounded relative motion at the chief orbit apoapses, we set $r(t_0) = r_a = a(1+e)$ and follow the same steps. The resulting constraint for chief orbits with a general eccentricity is

$$\frac{\dot{y}_0}{x_0} = \frac{-n(2-e)}{\sqrt{(1-e)(1+e)^3}} \tag{54}$$

while the constraint for chief orbits with a small eccentricty is given by

$$\dot{y}_0 + (2-3e)nx_0 = 0 \tag{55}$$

Note that if the chief orbit is circular and $e = 0$, then this bounded relative motion constraint reduces to the familiar form of

$$\dot{y}_0 + 2nx_0 = 0 \tag{56}$$

which is classically obtained by solving the Clohessy-Wiltshire differential equations. The more general bounded relative orbit constraint in Eq. (52) is valid for eccentric chief orbits. However, its form requires that t_0 be defined to be at the orbit perigee point.

If we include the J_2 perturbation, then the various orbit elements will experience short period, long period and secular drift.[26,27] Mapping the instanteneous osculating orbit elements to mean elements, only the ascending node, argument of perigee and mean anomaly will experience secular drifts. It was shown in References 8 and 9 that the following two mean orbit element constraints will make all orbits drift on average at the same angular rates $\dot{\theta}$ and $\dot{\Omega}$:

$$\delta\eta = -\frac{\eta}{4}\tan i\ \delta i \tag{57a}$$

$$\delta a = \frac{J_2}{2\eta^5}\left(4+3\eta\right)\left(1+5\cos^2 i\right)r_{eq}\delta\eta \tag{57b}$$

The scalar parameter r_{eq} is the equatorial Earth radius. Note that all orbit elements and orbit element differences in Eq. (57) are assumed to be mean states, not osculating states.[26] Whereas a Keplerian motion requires δa to be zero to obtain a repeating, closed relative orbit, if the J_2 induced orbit drift is also considered than δa must be non-zero if either a change in eccentricity or change in inclination is required. However, note that with this constraint the mean $\delta\dot{\theta}$ will be zero, but the mean $\delta\omega$ and δM will have secular drifts. The linearized relative motion predictions in Eqs. (22), (28), (33) or (39) should be treated as the mean relative motion where the short and long period components have been removed. Over one orbit the affect of the J_2 induced drift will be very small. As such, we can ignore the small drifts in the orbit element differences and simply hold them constant to evaluate the shape and geometry of relative orbit. To see the long term effect of the orbit elements drift (i.e. study multiple orbit revolutions), the orbit element differences $\delta\omega$ and δM must be considered to be slowly time varying.[9] Other orbit parameter constraints could be imposed as well, as long as these constraint will yield a bounded relative orbit.

Numerical Simulations

The following numerical simulations verify that the relative motion approximation in Eqs. (22), (33) and (39) do indeed predict the spacecraft formation geometry. These simulations also illustrate the accuracy at which these simplified linearized solutions are valid. Let the chief orbit be given by the orbit elements shown in Table 1.

Table 1 Chief Orbit Elements

Orbit Elements	Value	Units
a	7555	km
e	0.03 or 0.13	
i	48.0	deg
Ω	20.0	deg
ω	10.0	deg
M_0	0.0	deg

The relative orbits are studied for two different chief eccentricities. For the relative orbits studied, the ratio ρ/r is about 0.003. The smaller of the two eccentricities considered is already an order of magnitude larger than this, while the second eccentricities is even larger again. The numerical simulations show that the small eccentricity assumption (i.e. retaining terms in e but dropping higher order terms in e) will still yield a reasonable relative orbit prediction for $e = 0.03$, even though it is larger than the small term ρ/r. The orbit element differences which define the relative orbit are given in Table 2. Since these simulations assume a two-body Keplerian motion of the satellites, the semi-major axis difference δa must be zero to achieve a bounded relative motion.

Table 2 Orbit Element Differences Defining the Spacecraft Formation Geometry

Orbit Elements	Value	Units
δa	0	km
δe	0.00095316	
δi	0.0060	deg
$\delta\Omega$	0.100	deg
$\delta\omega$	0.100	deg
δM_0	-0.100	deg

The following figures compare the relative orbit motion for four different cases. Case 1 is the relative motion that will result using the true nonlinear equations of motion. Case 2 uses the dimensional linearized analytical relative orbit solution in Eq. (22). The only assumption that has been made here is that the ratio between the relative orbit radius ρ and the inertial chief orbit radius r is small and terms involving ρ/r have been dropped. Case 3 assumes that the chief orbit eccentricity is small, but not near zero. As such, higher order terms in e are dropped, while terms which depend linearly on e are kept. The relative orbit motion is described through Eq. (33). Case 4 assumes that the chief orbit is near-circular and that e is very close to zero. Any terms involving the eccentricity e are dropped here to yield the classical CW equations in Eq. (39). Case 4 is not included here to suggest that a circular orbit assumption should be made when the chief orbit is clearly eccentric. The circular chief orbit assumption case is included to provide a relative comparison illustrating the extent of the eccentricity effect.

The resulting relative orbit motion is illustrated in Figure 3. Figures 3(a) and 3(b) show the three-dimensional relative orbits for cases 1 through 4 as seen by the rotating Hill reference frame. The relative orbit radii vary betwen 10 and 20 kilometers. When $e = 0.03$, note that the relative orbits for cases 1–3 are virtually indistinguishable. Only the relative orbit prediction assuming a circular orbit (case 4) has a clearly distinct motion. Studying Figure 3(b) with $e = 0.13$, the case 2 relative orbit is still indistiniguishable on this scale from the true relative motion in case 1. With this larger eccentricity the relative motion predicted in case 3 (dropping higher order terms in e) does show some visible departure from the true relative motion. As expected, the circular chief orbit assumption (case 4) yields a very poor prediction of the relative orbit motion.

In Figures 3(c) and 3(d) the RMS relative orbit errors are shown in polar plots versus the chief orbit true anomaly. For the $e = 0.03$ simulations, the relative orbit errors for case 2 lie between 20 and 40 meters. Since the relative orbit radius is roughly 10 kilometers, this corresponds to a 0.2–0.4 percent relative motion error. The RMS relative motion error for case three is only marginally worse. As was discussed earlier, dropping the higher order e terms should begin to have a noticably affect on the relative motion errors. For the $e = 0.13$ simulations, the relative motion errors for case 2 lie between 50 and 100 meters (roughly 0.5–1.0 percent errors). However, dropping the higher order e terms in case 3 has a very noticable effect with the relative motion errors growing as large as 500 meters (about 5.0 percent error).

Conclusion

Analytical linearized relative orbit descriptions are provided for several types of chief orbit eccentricities where orbit element differences are chosen to define the relative orbit geometry. The relative orbit motion between a deputy and chief satellite is given in terms of the true anomaly difference. With these linearized relative motion solutions, it is trivial to estimate what the effect of changing a particular orbit element difference will be. Orbit element differences have the advantage that they are constants of the Keplerian two-body solution if the mean anomaly difference is selected as the relative anomaly measure. Assuming that a bounded relative orbit constraint is satisfied, then all six orbit element differences will remain constant. If the bounded relative orbit constraint is not satisfied, or there are other perturbations present such as the J_2 gravitational perturbations, then some or all of the orbit element differences will vary slowly with time. The presented analytical solutions in terms of the orbit element differences are still valid. However, care must be taken to treat the appropriate orbit element differences as time varying. The resuting relative orbit motion descriptions can be used both in spacecraft formation flying control developments, as well as in the relative orbit design phase. The relative orbit solutions are written such that their secular offset and sinusoidal motions are clearly separated. As such, it is easy to see what the offsets and sinusoidal amplitudes will be for a given set of orbit element differences in the orbit radial, along-track and out-of-plane motion.

Acknowledgment

I would like to thank Prof. K. T. Alfriend for the fruitful discussions that led to an enhanced version of this paper.

References

[1]Kechichian, J. and Kelly, T., "Analytical Solution of Perturbed Motion in Near-Circular Orbit Due to J2, J3 Earth Zonal Harmonics in Rotating and Inertial Cartesian Reference Frames," *AIAA 27th Aerospace Sciences Meeting*, Reno, Nevada, January 1989, Paper No. 89-0352.

[2]Kechichian, J. A., "The Analysis of the Relative Motion in General Elliptic Orbit with Respect to a Dragging and Precessing Coordinate Frame," *AAS/AIAA Astrodynamics Specialist Conference*, Sun Valley, Idaho, August 1997, Paper No. 97-733.

[3]Queiroz, M. S. D., Kapila, V., and Yan, Q., "Nonlinear Control of Multiple Spacecraft Formation Flying," *Proceedings of AIAA Guidance, Navigation, and Control Conference*, Portland, OR, Aug. 1999, Paper No. AIAA 99–4270.

[4]Sedwick, R., Miller, D., and Kong, E., "Mitigation of Differential Perturbations in Clusters of Formation Flying Satellites," *AAS/AIAA Space Flight Mechanics Meeting*, February 1999, Paper No. AAS 99-124.

[5]Melton, R. G., "Time-Explicit Representation of Relative Motion Between Elliptical Orbits," *Journal of Guidance, Control, and Dynamics*, Vol. 23, No. 4, 2000, pp. 604–610.

[6]Tschauner, J. and Hempel, P., "Rendezvous zu einem in Elliptischer Bahn Umlaufenden Ziel," *Astronautica Acta*, Vol. 11, 1965, pp. 104–109.

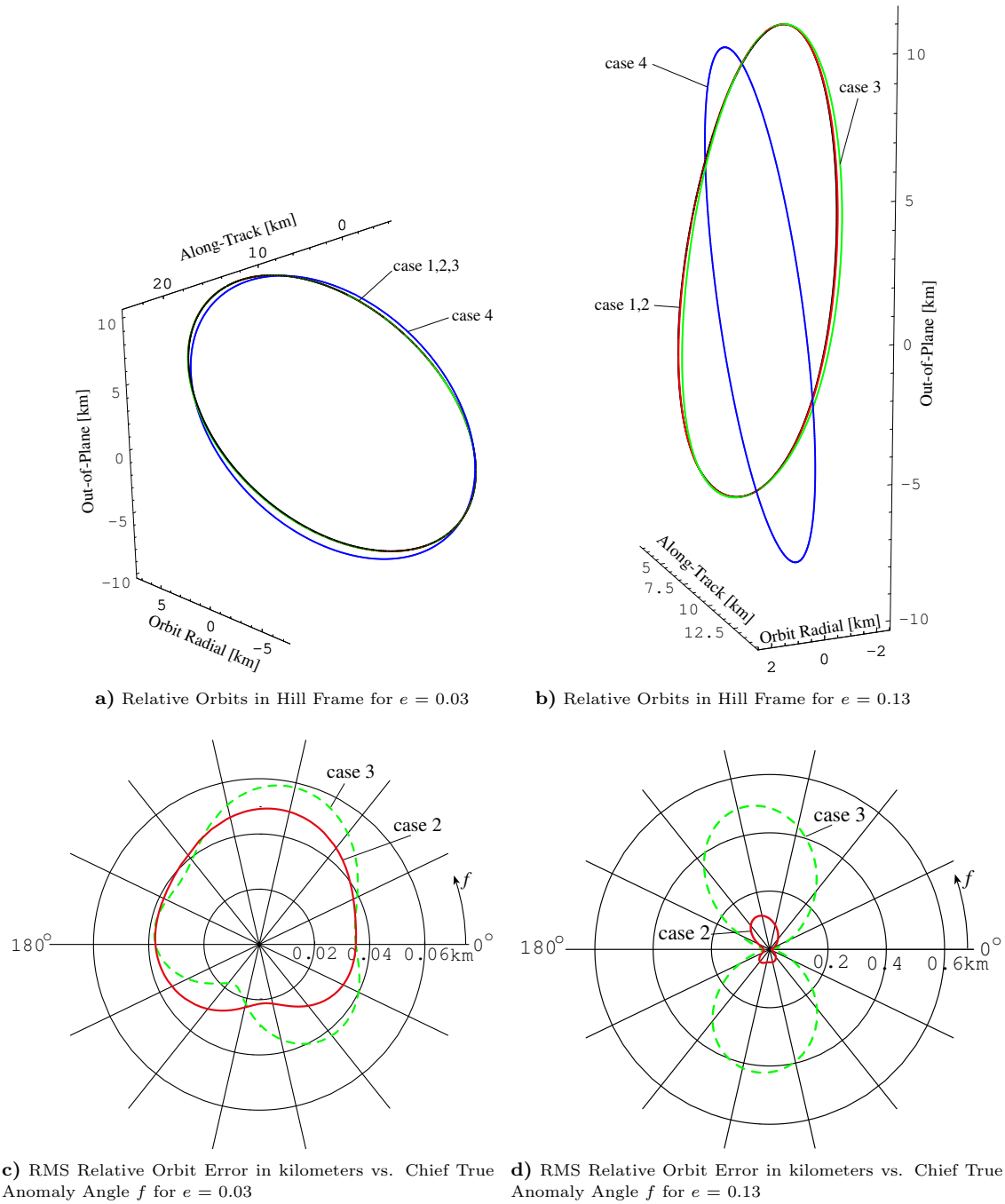

a) Relative Orbits in Hill Frame for $e = 0.03$

b) Relative Orbits in Hill Frame for $e = 0.13$

c) RMS Relative Orbit Error in kilometers vs. Chief True Anomaly Angle f for $e = 0.03$

d) RMS Relative Orbit Error in kilometers vs. Chief True Anomaly Angle f for $e = 0.13$

Fig. 3 Comparison of the Linearized Relative Orbit Solutions for Cases 1–4 with $e = 0.03$ and $e = 0.13$.

[7]Broucke, R. A., "A Solution of the Elliptic Rendezvous Problem with the Time as Independent Variable," *AAS/AIAA Space Flight Mechanics Meeting*, San Antonio, TX, January 2002, Paper No. AAS 02-144.

[8]Schaub, H. and Alfriend, K. T., "J_2 Invariant Reference Orbits for Spacecraft Formations," *Celestial Mechanics and Dynamical Astronomy*, Vol. 79, 2001, pp. 77–95.

[9]Alfriend, K. T. and Schaub, H., "Dynamics and Control of Spacecraft Formations: Challenges and Some Solutions," *Journal of the Astronautical Sciences*, Vol. 48, No. 2 and 3, April–Sept. 2000, pp. 249–267.

[10]Garrison, J. L., Gardner, T. G., and Axelrad, P., "Relative Motion in Highly Elliptic Orbits," *AAS/AIAA Space Flight Mechanics Meeting*, Albuquerque, NM, Feb. 1995, Paper No. 95-194.

[11]Chichka, D. F., "Satellite Cluster with Constant Apparent Distribution," *Journal of Guidance, Control and Dynamics*, Vol. 24, No. 1, Jan.–Feb. 2001, pp. 117–122.

[12]Hughes, S. P. and Hall, C. D., "Optimal Configurations of Rotating Spacecraft Formations," *Journal of the Astronautical Sciences*, Vol. 48, No. 2 and 3, April–Sept. 2000, pp. 225–247.

[13]Schaub, H., Vadali, S. R., and Alfriend, K. T., "Spacecraft Formation Flying Control Using Mean Orbit Elements," *Journal of the Astronautical Sciences*, Vol. 48, No. 1, 2000, pp. 69–87.

[14]Tan, Z., Bainum, P. M., and Strong, A., "The Implementation of Maintaining Constant Distance Between Satellites in Elliptic Orbits," *AAS Spaceflight Mechanics Meeting*, Clearwater, Florida, Jan. 2000, Paper No. 00-141.

[15]Schaub, H. and Alfriend, K. T., "Impulsive Feedback Control to Establish Specific Mean Orbit Elements of Spacecraft Formations," *Journal of Guidance, Control and Dynamics*, Vol. 24, No. 4, July–Aug. 2001, pp. 739–745.

[16]Schaub, H. and Alfriend, K. T., "Hybrid Cartesian and Orbit Element Feedback Law for Formation Flying Spacecraft," *Journal of Guidance, Control and Dynamics*, Vol. 25, No. 2, March–April 2002.

[17]Naasz, B. J., *Classical Element Feedback Control for Spacecraft Orbital Maneuvers*, Master's thesis, Virginia Polytechnic Institute and State University, Blacksburg, VA, May 2002.

[18]Alfriend, K. T., Schaub, H., and Gim, D.-W., "Gravitational Perturbations, Nonlinearity and Circular Orbit Assumption Effect on Formation Flying Control Strategies," *AAS Guidance and Control Conference*, Breckenridge, CO, February 2000, Paper No. AAS 00-012.

[19]Gim, D.-W. and Alfriend, K. T., "The State Transition Matrix

of Relative Motion for the Perturbed Non-Circular Reference Orbit," *AAS/AIAA Space Flight Mechanics Meeting*, Santa Barbara, CA, Feb. 2001, Paper No. 01-222.

[20]Hill, G., "Researches in the Lunar Theory," *American Journal of Mathematics*, Vol. 1, 1878, pp. 5–26.

[21]DeVries, J. P., "Elliptic Elements in Terms of Small Increments of Position and Velocity Components," *AIAA Journal*, Vol. 1, No. 9, Nov. 1963, pp. 2626–2629.

[22]Beyer, W. H., *Standard Mathematical Tables*, CRC Press, Inc., West Palm Beach, Fl., 1974.

[23]Hughes, S. P. and Mailhe, L. M., "A Preliminary Formation Flying Orbit Dynamics Analysis for Leonardo-BRDF," *IEEE Aerospace Conference*, Big Sky, Montana, March 11–17 2001.

[24]Clohessy, W. H. and Wiltshire, R. S., "Terminal Guidance System for Satellite Rendezvous," *Journal of the Aerospace Sciences*, Vol. 27, No. 9, Sept. 1960, pp. 653–658.

[25]Inalhan, G. and How, J. P., "Relative Dynamics & Control of Spacecraft Formations in Eccentric Orbits," *Journal of Guidance, Control and Dynamics*, Vol. 25, No. 1, Jan.–Feb. 2002, pp. 48–59.

[26]Brouwer, D., "Solution of the Problem of Artificial Satellite Theory Without Drag," *The Astronomical Journal*, Vol. 64, No. 1274, 1959, pp. 378–397.

[27]Battin, R. H., *An Introduction to the Mathematics and Methods of Astrodynamics*, AIAA Education Series, New York, 1987.